Fatigue performance of friction stir welded marine grade steel

Helena Polezhayeva[a], Athanasios I. Toumpis[b*], Alexander M. Galloway[b], Lars Molter[c], Bilal Ahmad[d], Michael E. Fitzpatrick[e]

[a]*Independent Consultant, 78 New Road, Chilworth, GU4 8LU, United Kingdom*

[b]*Department of Mechanical & Aerospace Engineering, University of Strathclyde, James Weir Building, 75 Montrose Street, Glasgow G1 1XJ, United Kingdom*

[c]*Center of Maritime Technologies e.V., Bramfelder Str. 164, D-22305, Hamburg, Germany*

[d]*Materials Engineering, Department of Engineering and Innovation, The Open University, Walton Hall, Milton Keynes, MK7 6AA, United Kingdom*

[e]*Faculty of Engineering and Computing, Coventry University, Priory Street, Coventry CV1 5FB, United Kingdom*

Abstract

An extensive study on the fatigue performance of friction stir welded DH36 steel was carried out. The main focus of this experimental testing programme was fatigue testing accompanied by tensile tests, geometry measurements, hardness and residual stress measurements, and fracture surface examination. The *S-N* curve for friction stir butt welded joints was generated and compared with the International Institute of Welding recommendations for conventional fusion butt welds. Friction stir welds of marine grade steel exceeded the relevant rules for fusion welding. This newly developed *S-N* curve is being proposed for use in the relevant fatigue assessment guidelines for friction stir welding of low alloy steel. Fracture surfaces were examined to investigate the fatigue failure mechanism, which was found to be affected by the processing features generated by the friction stir welding tool.

Keywords: Friction stir welding; Low alloy steel; Fatigue testing; Residual stresses; Fracture surface analysis.

* Corresponding author. Tel.: +44 0141 574 5075
e-mail address: athanasios.toumpis@strath.ac.uk

1. Introduction

Fatigue cracking in welded joints of structural components is a major cause of structural failure [1]. Therefore, most welded structures that are expected to experience fatigue loading are designed to satisfy fatigue strength requirements [2,3]. The cracks in conventional fusion welds are triggered by stress concentration due to changes of geometry, welding defects such as undercut, porosity, lack of fusion, cold laps etc., as well as residual stress, mechanical in-homogeneity and misalignments [3,4]. Satisfactory fatigue performance is achieved, among other means, by reduction in stress concentration of welded joints.

Friction stir welding (FSW) is an innovative welding technique which was patented by The Welding Institute and first introduced in 1991 [5]. Since its invention, the technique has mostly been used for aluminium alloys. Research has demonstrated the superior fatigue performance of FSW joints in aluminium as compared to those produced by fusion welding [6-8] due to significantly reduced stress concentration at a joint compared with fusion welding techniques.

A study [8] examined the influence of welding speed on fatigue strength of Al–Mg–Si alloy 6082. It was concluded that using a welding speed within the industrially accepted range has no major influence on the mechanical and fatigue properties of the FSW. However the fatigue performance of FSW was significantly improved at a very low welding speed, which is attributed to the increased thermal energy supplied to the weld per unit length. The results of fatigue testing of FSW were also compared with those for conventional arc-welding methods; MIG-pulse and TIG (Metal Inert Gas and Tungsten Inert Gas, respectively). The MIG-pulse and TIG welds showed lower static and fatigue strength than that of FSW. The effect of the welded surface finishing treatment on the fatigue behaviour of AA8090 FSW butt joints was studied by another publication [9] where the specimens subjected to surface finishing treatment demonstrated better fatigue performance as compared with the as-welded specimens.

The number of publications on the fatigue performance of FSW in low alloy steel is limited to those discussed herein. A study on FSW of DH36 steel was carried out to evaluate the mechanical properties (including fatigue strength) of the welds with a view to its possible application in the shipbuilding industry [10]. The researchers [10] investigated FSW of 4, 6 and 8 mm thick DH36 steel as compared with submerged arc welds. The conclusion was drawn on superior fatigue performance of FSW. It was also found that two FSW passes, one from either side, result in significant improvement in fatigue strength compared with that of single pass FSW [10]. Fatigue testing, tensile testing and hardness measurements were performed on double sided friction stir welds of S275 structural steel [11], where welding was carried out in air and underwater. It was shown that FSW carried out in air and underwater produced similar fatigue properties [11].

FSW of 4 mm thick GL-A36 steel was investigated with the purpose of evaluating the process for shipbuilding applications [12]. The fatigue resistance of parent material and FSW produced using various welding parameters, pre-welding conditions and tools were compared. The fatigue behaviour of FSW was similar to that of the parent material [12]. The fatigue properties of friction stir welded AISI 409M grade ferritic stainless steel joints were studied elsewhere [13]. FSW demonstrated improved fatigue behaviour compared with the parent material, including crack propagation stage. This was attributed to the FSW dual phase, ferritic–martensitic microstructure, superior tensile properties and favourable residual stresses [13].

The marine and offshore industries face demands for increased service lives of offshore structures, so this makes FSW of steel a very promising technique as it allows to reduce local stress concentration therefore improve fatigue performance. Still, in order to offer steel FSW to

industry as an alternative to fusion welding, the existing knowledge gap on the fatigue behaviour of steel FSW must be addressed. The current research advances the scientific understanding of steel FSW by developing novel *S-N* curve parameters with respect to low alloy steel for marine applications. For this purpose, an extensive industrial scale testing programme was undertaken, including fatigue and tensile testing, hardness and residual stress measurements, and examination of fracture surfaces. The latter is performed to relate the fatigue failure to the FSW microstructure and investigate the mechanism for crack initiation and propagation. The *S-N* curve for FSW in low alloy steel was constructed and compared to IIW recommendations [3] and the effect of longitudinal and transverse residual stresses has been assessed.

2. Experimental programme

2.1. Material and welding details

The test specimens were produced from 6 mm thick marine grade DH36 steel. This particular steel grade is widely used in ship structures, especially in stiffened panels. The chemical composition of DH36 as provided by the steel manufacturer is given in Table 1. The minimum acceptable mechanical properties for DH36 steel of thicknesses ≤ 50 mm according to Lloyd's Register rules [14] are outlined in Table 2.

Table 1. Chemical composition of 6 mm thick DH36 steel (wt%)

C	Si	Mn	P	S	Al	Nb	N
0.11	0.37	1.48	0.014	0.004	0.02	0.02	0.002

Table 2. Minimum acceptable mechanical properties of 6 mm thick DH36 steel [14]

Grade	Yield Strength N/mm^2	Tensile Strength N/mm^2	Elongation, %	Charpy V-notch Impact tests	
				Average Energy at -20^{0}C, J	
				Longitudinal	Transverse
DH36	355	490-620	21	34	24

Steel plates of 2000 mm x 200 mm x 6 mm were butt welded using a MegaStir Q70 pcBN-WRe tool for steel with scrolled shoulder (dia. 36.8 mm) and stepped spiral probe (5.7 mm length). FSW was performed at varying traverse and rotational speeds as indicated in Table 3. Each combination of traverse and rotational speed from Table 3 will further be referred to as 'slow', 'intermediate' and 'fast' welding speed. The welding speed combinations were selected as representative of a previous research [15].

Table 3. Welding parameter sets

Welding speed group	Slow	Intermediate	Fast
Traverse speed (mm/min)	100	250	500
Rotational speed (rpm)	200	300	700

Metallographic examination of the welds produced using slow, intermediate and fast speed has been discussed previously [16]. It was demonstrated that slow speed welding delivers a homogeneous microstructure with significant grain refinement in comparison to the parent material [16].

2.2. Specimens

The specimens for fatigue and tensile tests were transversely machined from welded plates. The shape and dimensions of the specimens are shown in Figure 1.

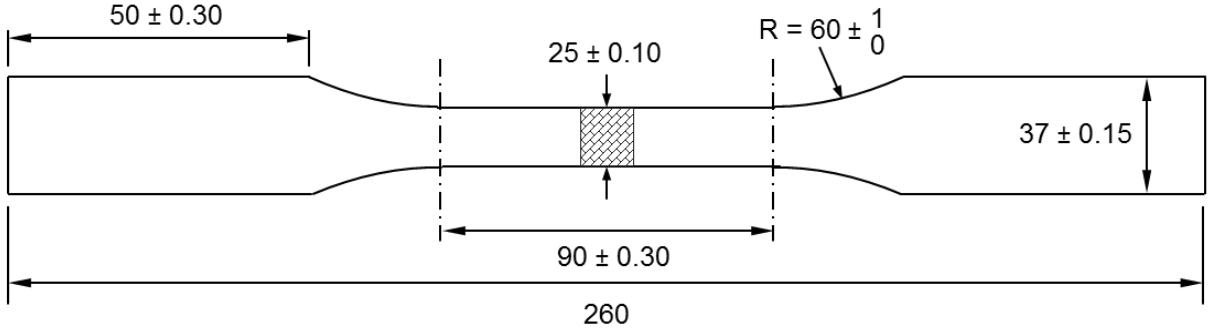

Figure 1. Transverse fatigue and tensile test specimens (dimensions in mm), 6 mm thick

The specimen sides were polished up to a surface finish of 0.2 μm R_a or better, according to the applicable British Standards [17] to avoid fatigue crack initiation from the machining marks. To ensure that the required surface roughness was achieved, surface roughness measurements were performed using a Mitutoyo system. The top and bottom surfaces of the specimens (where the top surface is the tool contact surface) were left in the as-welded condition, and a subsequent assessment of the linear and angular misalignment (distortion) showed that these were negligible.

Three specimens per weld speed were subjected to tensile testing in order to identify the yield strength (YS) of the weldments. The average YS value for the intermediate weld speed was 382 MPa; this value was used to calculate the applied loads for fatigue testing.

2.3. Hardness measurements

A homogeneous hardness distribution in welds is important from a fatigue point of view as abrupt changes in hardness produce a material notch [18]. Average hardness values were measured in FSW sections for each of the slow, intermediate and fast welds. The positions for measurements representative of the weld zone are given in Figure 2. The measurements were taken using a Mitutoyo hardness tester by applying a load of 200 gf.

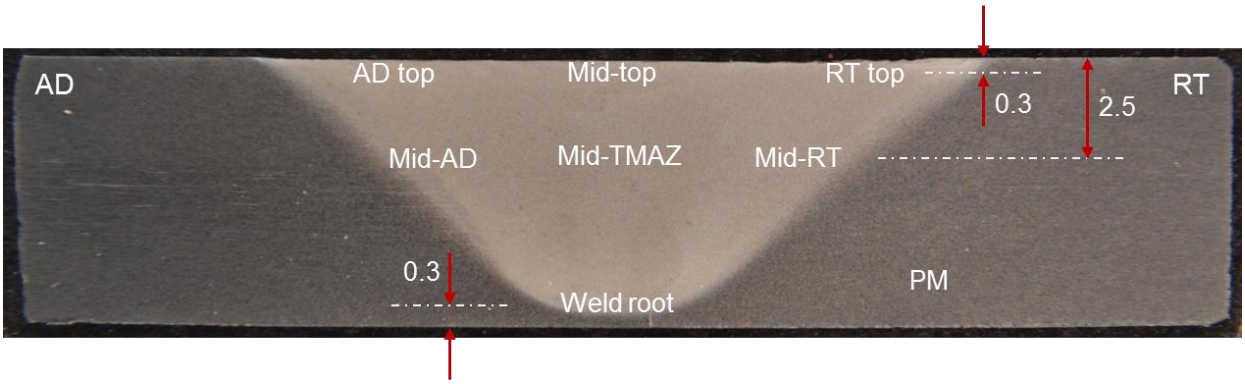

Figure 2. Hardness measurement positions in FSW transverse section

The hardness measurements for the three weld speeds are presented in Figure 3, where the values are supplied as an average of two measurements per position marked in Figure 2. In all relevant figures, AD and RT correspond to the advancing and retreating side of the weld respectively, whereas HAZ is the heat affected zone and TMAZ is the thermo-mechanically affected zone. As seen from Figure 3, the steel that is affected by the welding process is harder than the parent material. In addition, the hardness of the weld is increased with increasing welding speed. This can be attributed to the increasing cooling rate which causes the development of harder phases such as bainite. Microstructural examination [15,16] has discussed the rise in bainite content with each speed increment.

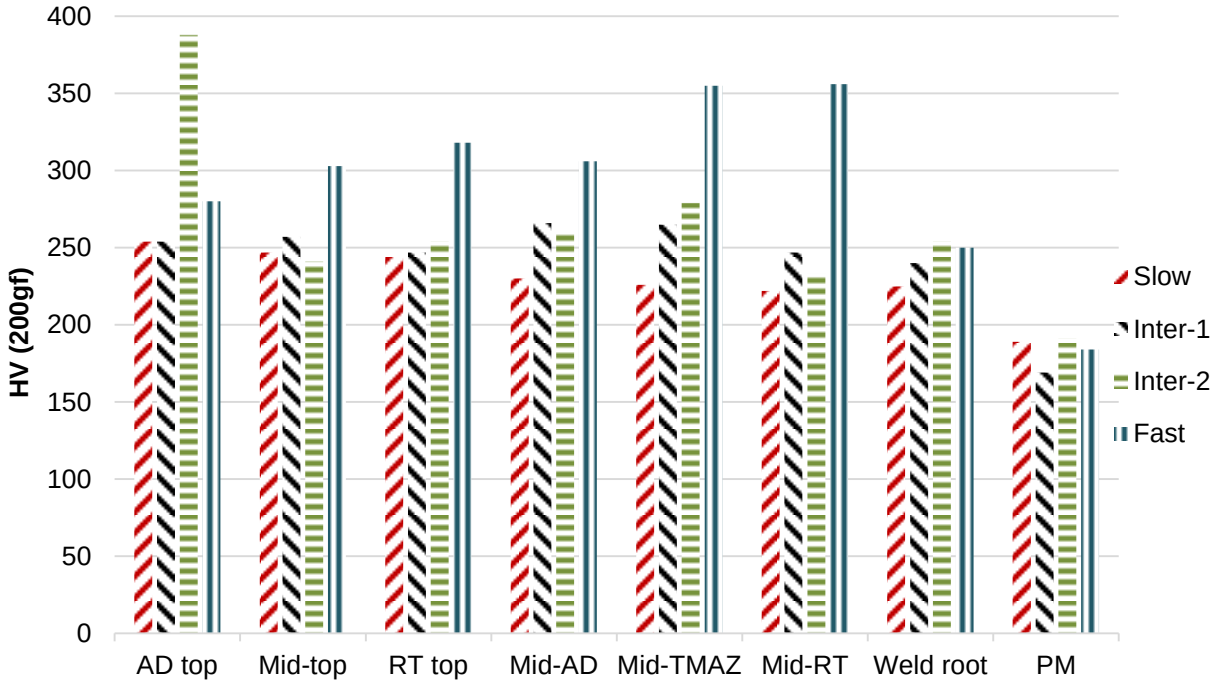

Figure 3. Hardness distribution for three welding speeds

2.4. Residual stress measurements

The sample for residual stress measurements was transversely machined from a welded plate of 6 mm thickness. Figure 4 shows the top surface of an examined weld section of approx. 400 mm (width) x 230 mm (length).

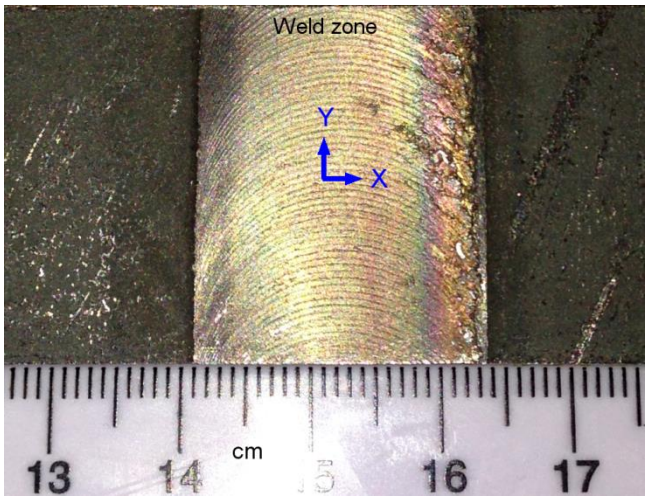

Figure 4. The weld top surface of a sample for residual stress measurements (welding direction is top to bottom)

X-Ray diffraction (XRD) measurements were carried out using a Stresstech XStress3000 X-Ray diffractometer; results were extracted using the $\sin^2\psi$ technique [19]. A 3-mm-diameter collimator was used with X-Ray exposure time of 10 seconds for each ψ tilt. The angle ψ, defining the orientation of the sample surface, is the angle between the normal of the surface and the incident and diffracted beam bisector. Residual stress measurements were performed across the weld zone. The measured locations are shown in Figure 5.

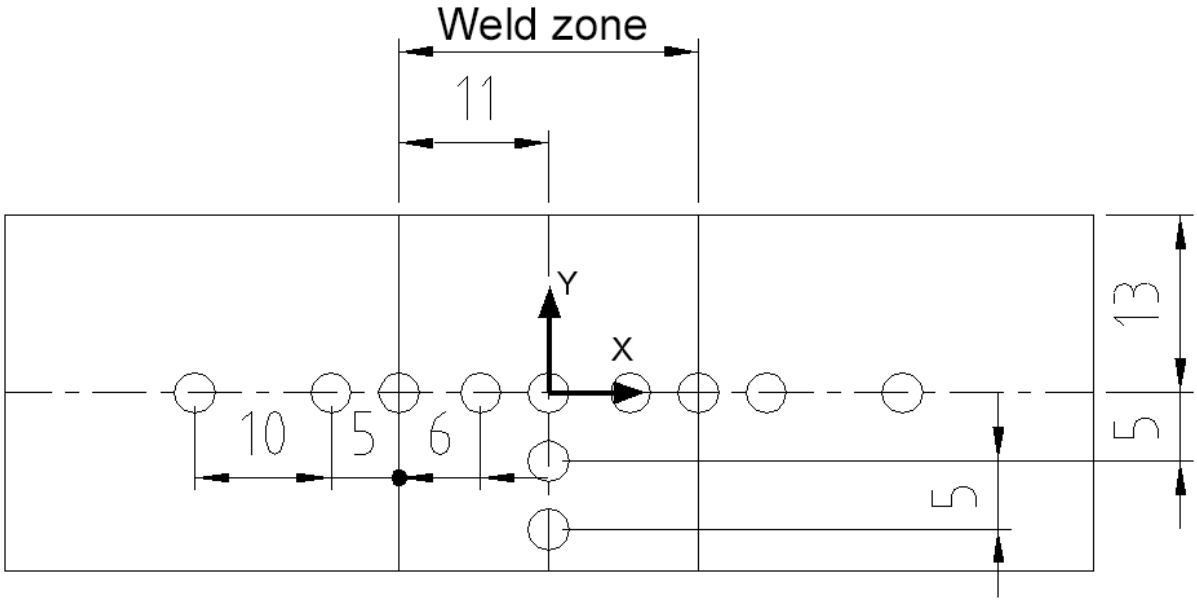

Figure 5. Locations and directions of residual stress measurements (each circle indicates the diameter of the collimator, dimensions in mm)

Figures 6 and 8 show the residual stress profile for the slow speed weld, for top surface side and weld root side (top and bottom of weld) respectively. As seen from Figure 6, the maximum transverse residual stress is close to YS and is located in the central stir zone of the weld. In the HAZ where fatigue cracking is generally expected to initiate [18] due to increased stress concentration [20], change in the local microstructure and altered physical properties [21], the residual stress is approx. 100-150 MPa. Therefore, the locations of the maximum residual stress and of the possible crack initiation site are separated. This is yet another reason for the improved fatigue performance of FSW as compared with fusion welds where the maximum

transverse residual stress, close to the material's YS, is observed at the weld toe [20] and leads to crack initiation at that location.

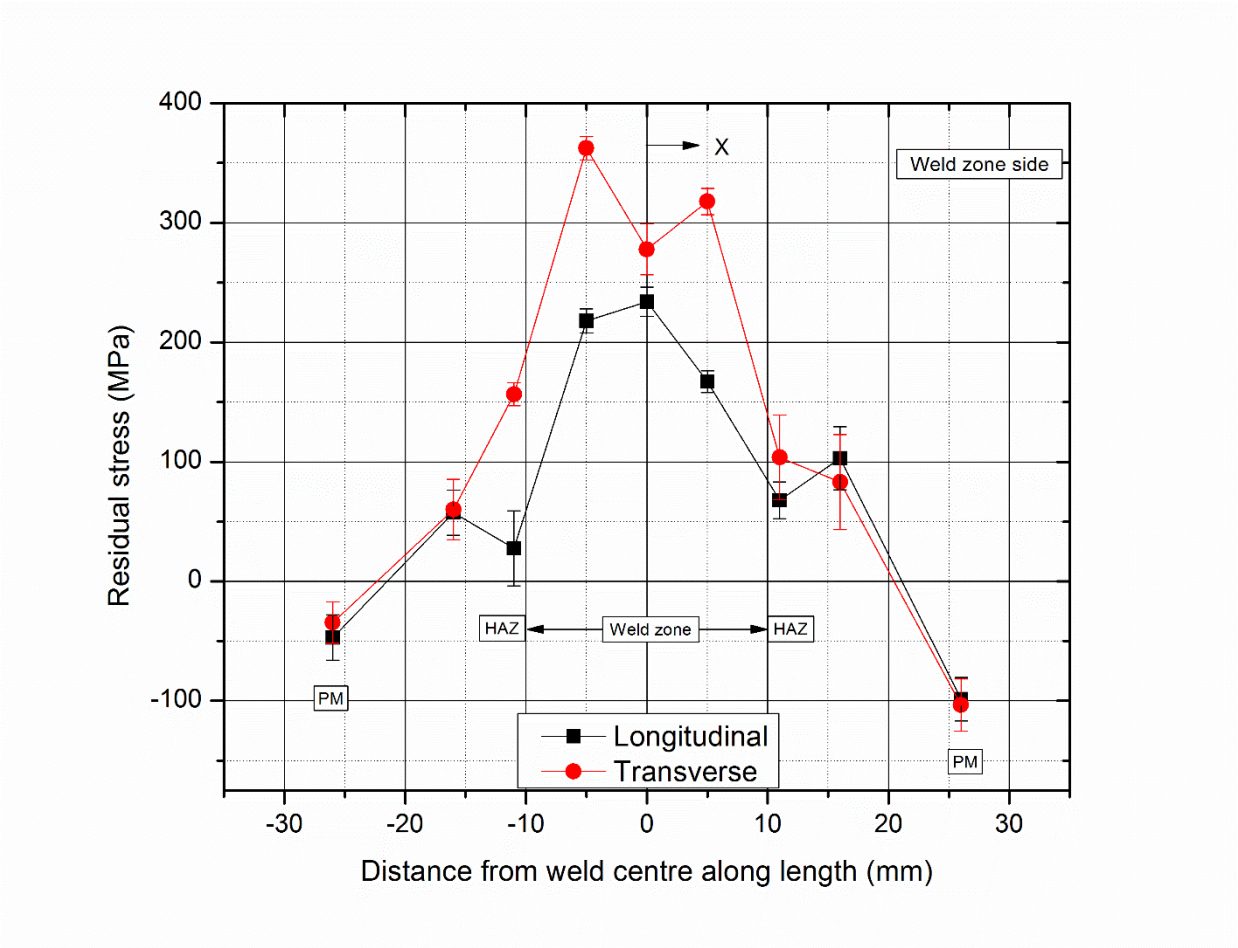

Figure 6. Residual stress profile for slow speed weld, top surface side

In the specimen's HAZ, a split in data was seen from the negative and positive ψ tilts (Figure 7). During XRD measurements, a split in data from both ψ tilts can occur due to the presence of shear stress [22]. This displays that the HAZ region has high magnitude of shear stress as compared to the TMAZ. Figure 8 reveals that the transverse residual stress on the weld root side of the specimen is lower than on the top surface side and compressive in the weld root.

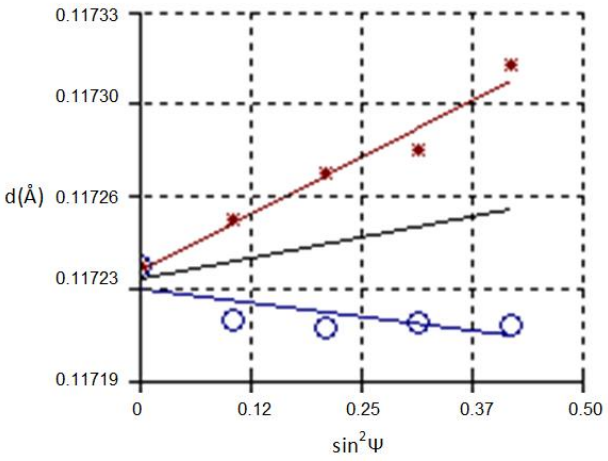

Figure 7. Splitting of d vs $\sin^2\psi$ plot in the HAZ region

Residual stress is one of the significant factors that affect the fatigue life of welded structural members; it is well known that tensile residual stress decreases fatigue life. Improvements in the welding processes have reduced the associated tensile residual stress to some extent. Fatigue cracks are typically seen to initiate at locations which exhibit high tensile residual stress, stress concentration or weld defects. In the case of fillet [23] and butt [24] joints with fusion welds, fatigue cracks were seen to initiate at the weld toe owing to the combined effect of tensile residual stress and stress concentration. In the current study, the maximum tensile residual stress of the examined sample is located in the central weld zone hence not contributing to the fatigue failure. The friction stir weld zone exhibits higher surface roughness than the parent metal as a result of the processing features generated by the FSW tool. As outlined in Table 5, the predominant crack initiation site for the intermediate speed weld (24 out of 25 samples) is the weld edge; thus, the transition region between parent metal and weld zone acts as a notch and produces a correspondingly high stress concentration factor initiating failure.

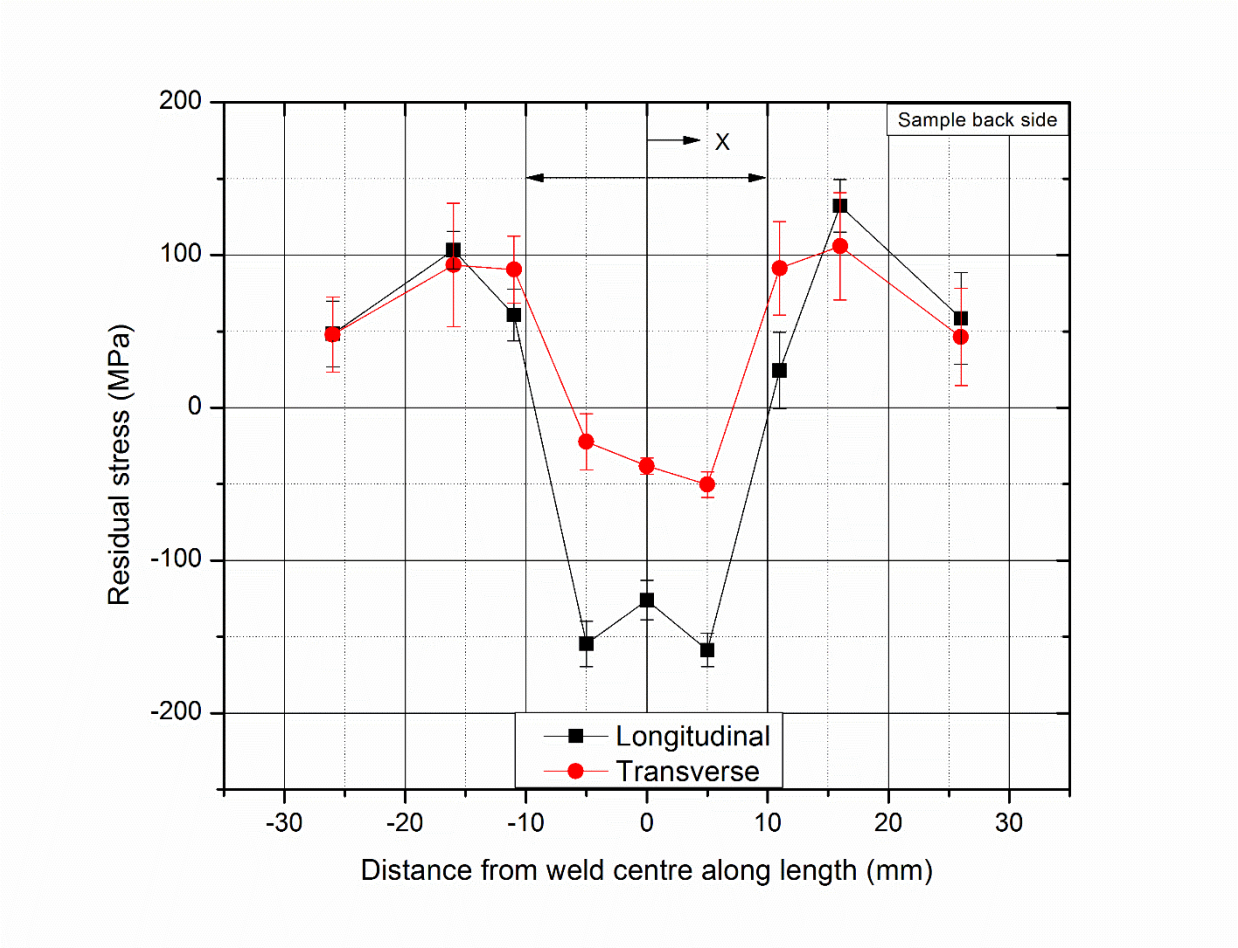

Figure 8. Residual stress profile, weld root

2.5. Fatigue testing

Fatigue testing was carried out on an Instron 8802 fatigue testing system. The number of tested specimens per welding speed and stress range is outlined in Table 4. The specimens produced using the intermediate weld speed were selected for the construction of the *S-N* curve. The intermediate speed is considered to be optimal based on research reported in an earlier work [15]. The term “optimal” reflects the balance between commercially competitive production speed (compared to fusion welding) and high integrity welds that this welding speed had

demonstrated. Although having exhibited the best results in terms of weld quality and mechanical properties [15], the slow traverse speed of 100 mm/min is clearly unrealistic in a real-world industrial environment. The effect of varying welding speed on the fatigue performance was established by testing the slow and fast weld speed specimens at one stress range and comparing these results with the basic *S-N* curve of the intermediate weld.

Table 4. Number of tested fatigue specimens per welding speed

Weld speed	Stress range (% of YS)	Number of tested samples
Intermediate	90	10
	80	10
	70	5
Slow	80	8
Fast	80	8

During the fatigue testing the stress ratio was maintained approx. equal to 0.1 and the stress frequency constant at 10 Hz.

3. Fatigue test results and analysis

The results of the fatigue tests are summarised in Table 5 together with the crack initiation sites. The nominal stress was calculated as applied load divided by net cross sectional area. The crack initiation site for 24 out of the 25 specimens of the intermediate weld (250 mm/min) was the weld edge on the RT side. The typical failure position can be seen in the photograph of a fractured specimen (Figure 9). The cracks initiated from lap defects observed on the RT side, as exhibited in Figure 13, Section 4. Minor embedded flaws detected on the AD side did not cause crack initiation.

Two specimens welded with slow speed (100 mm/min) did not fracture; the tests were terminated at 2.5×10^6 cycles and considered as run-outs. One specimen failed at approximately 4.2×10^5 cycles on the AD side of the weld; this was due to the incomplete fusion paths observed in this section of the weld. Two fast (500 mm/min) weld specimens had fatigue crack initiation from the weld root flaw; the third failed from the lap defect. A discussion on the fatigue failure mechanisms is provided in Section 4.

Table 5. Fatigue test results

Weld speed	Stress range, MPa	Number of cycles to failure	Crack initiation site[a]
Intermediate speed	265.83	479,985	Weld edge, RT
	261.78	602,646	Weld edge, RT
	263.81	1,116,339	Weld edge, RT

	263.94	1,967,444	Weld edge, RT
	262.19	589,711	Weld edge, RT
	264.00	1,114,315	Weld edge, RT
	263.09	317,472	Weld edge, RT
	262.61	941,637	Weld edge, RT
	262.68	1,899,174	Weld edge, RT
	261.71	678,298	Weld edge, RT
	296.96	310,992	Weld edge, RT
	298.81	335,264	Weld edge, RT
	296.83	254,089	Weld edge, RT
	296.29	359,445	Weld edge, RT
	295.01	337,432	Weld edge, RT
	296.96	312,883	Weld edge, RT
	295.41	350,413	Weld edge, RT
	296.29	629,054	Weld edge, RT
	296.42	664,426	Weld edge, RT
	295.48	492,379	Weld edge, RT
	230.67	1,489,360	Weld edge, RT
	228.72	2,600,000	Run out
	229.51	2,020,530	Weld edge, RT
	227.93	1,384,622	Weld edge, RT
	229.32	2,210,534	Weld edge, RT
	266	422,074	Weld stir zone, AD
	265.64	2,700,000	Run out
	265.21	2,500,000	Run out
Slow speed	264.55	2,612,700	Run out
	265.14	1,083,669	Weld stir zone, AD
	266.06	2,515,000	Run out
	262.19	2,520,000	Run out

	265.81	2,571,600	Run out
Fast speed	265.14	416,112	Weld root[b]
	262.13	222,272	Weld stir zone, AD
	264.29	722,691	Weld root[b]
	261.84	570,815	Weld root[b]
	263.39	129,490	Weld stir zone, AD
	261.59	731,208	Weld root[b]
	264.36	136,844	Weld stir zone, AD
	261.36	516,949	Weld root[b]

[a] In all relevant cases, the crack initiated at the top surface boundary of the tool stir marks.
[b] Crack propagated from the weld root flaw.

The fatigue test results in terms of nominal stress range against number of cycles to failure are plotted in Figure 10 in double logarithmic co-ordinates. The nominal *S-N* data for the intermediate weld from Table 5 and Figure 10 were analysed assuming a linear *S-N* curve on a log-log scale and using Equation 1:

$$\log N = \log A - m \times \log S \quad (1)$$

where S is the applied stress range, N is the fatigue life, and m and A are constants obtained experimentally. The run out test was not considered in this analysis. Initially, the inverse slope of the *S-N* curve was assumed as m=3.0. A statistical evaluation of parameter A at 50% and 97.7% of probability of survival, and standard deviation was performed according to IIW recommendations [3,25].

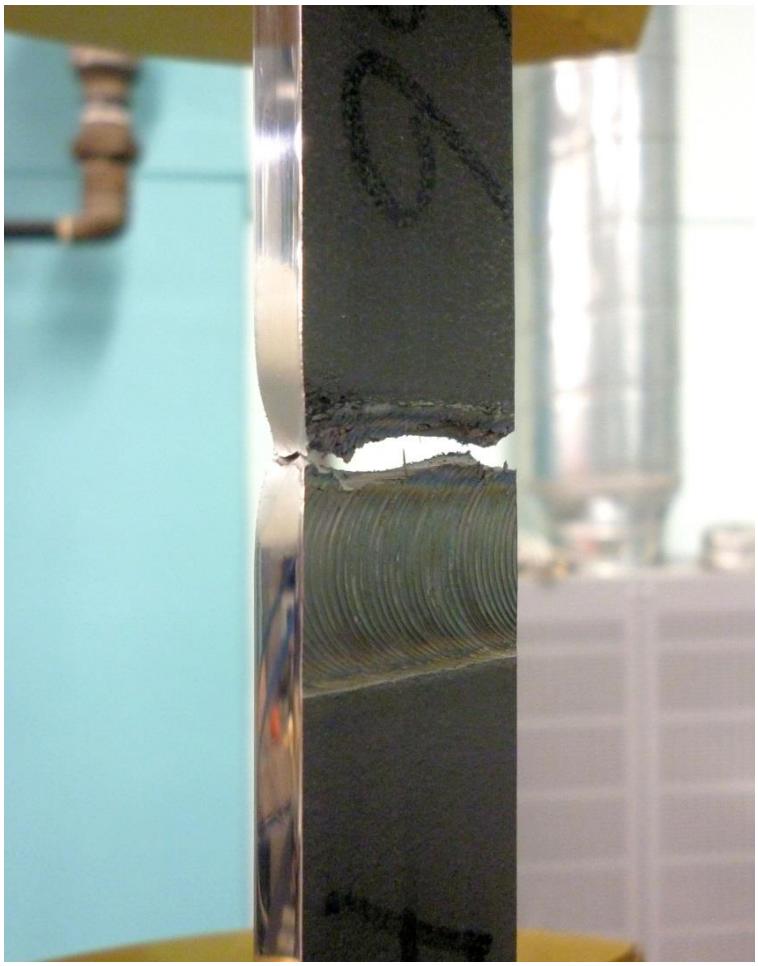

Figure 9. Typical failure position of intermediate weld specimen

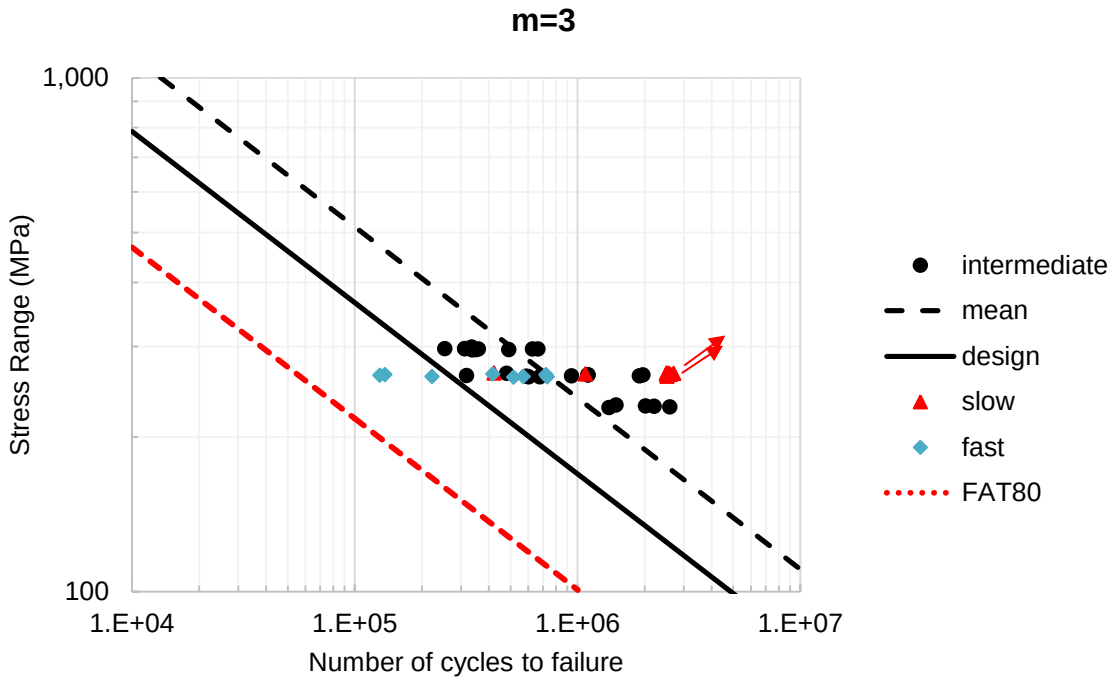

Figure 10. *S-N* data for the intermediate weld, inverse slope m=3

Figure 10 displays the *S-N* curves for the intermediate speed weld. The solid and dashed lines represent the probability of survival at 97.7% (design) and at 50.0% (mean), respectively. This *S-N* curve is compared with that recommended by IIW for fusion welds [3]. The detail most relevant to this investigation is the transverse single sided butt weld, Catalogue No. 214 [3]. The dotted line in Figure 10 indicates the IIW FAT 80 weld detail class at 97.7% probability of survival. The results for FSW demonstrate higher fatigue strength for all specimens of the intermediate weld in comparison to the FAT 80 class. The fatigue strength of the intermediate speed weld is FAT 135; this is 68% higher than the strength stated in the IIW Recommendations, FAT 80.

Further, there is a substantial scatter of the results (T_N) for the intermediate weld speed if an inverse slope of m=3 is used for *S-N* curve derivation, calculated according to Hobbacher [3] as:

$T_N = 1: (N_{10} / N_{90}) = 3.7$

where N_X is the number of cycles to failure at the x probability level of survival. The same applies to the scatter in terms of stress range T_σ, defined as [3]:

$T_\sigma = 1: (\sigma_{n10} / \sigma_{n90}) = 1.55$

where σ_{nx} is the stress range at the stated probability level of survival. The corresponding IIW recommended values are T_N=3.0 and T_σ=1.5 [3]. The calculated parameters T_N and T_σ indicate that the statistical analysis with a fixed slope of m=3 is not the most suitable. Indeed, best fit statistical evaluation based on IIW recommendations [3] produces an inverse slope of m=5.96.

It is therefore proposed to carry out the statistical analysis with assumed inverse slope of m=5 which is chosen based on IIW draft recommendations for weld improvement techniques [26]. The mean and design *S-N* curves with assumed inverse slope of m=5 and experimental data are shown in Figure 11. The scatter of fatigue test results for inverse slope of m=5 is characterised by T_N=3 and T_σ=1.25.

Table 6 provides the *S-N* curve parameters including design fatigue strength at $2x10^6$ cycles and standard deviation obtained for intermediate speed FSW using best fit, m=3 and m=5 assumptions. The design fatigue strength at $2x10^6$ cycles is above the parent material *S-N* curve FAT160 (m=5) [3]. This confirms that the use of the intermediate speed weld is the most appropriate for the derivation of the *S-N* curve.

Table 6. *S-N* curve parameters for intermediate speed weld

m	Mean A	Design A	Standard deviation	Fatigue strength at $2x10^6$ cycles, MPa
3	$1.35x10^{13}$	$4.87x10^{12}$	0.22	135
5	$9.86x10^{17}$	$4.11x10^{17}$	0.19	183
Best fit, 5.96	$2.17x10^{20}$	$9.06x10^{19}$	0.19	196

As can be seen from Figures 10 and 11, the results for slow and fast speed welds are consistent with the corresponding results obtained for aluminium by a separate study [8]; the slow welding speed results in better fatigue performance. This is because the slow speed produces a highly refined, homogeneous and defect-free microstructure as reported in a prior study [15].

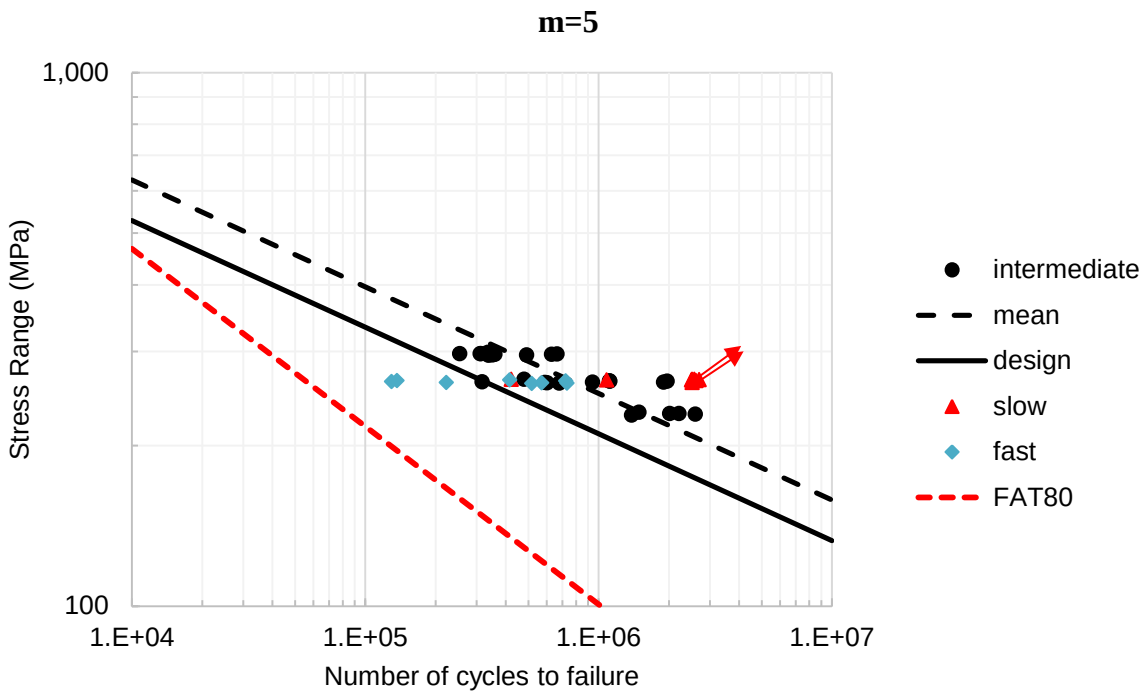

Figure 11. *S-N* data for the intermediate weld, inverse slope m=5.

4. Fracture surface analysis

The typical fracture surface for the intermediate weld specimens is shown in Figure 12 where a recurrent pattern of crack initiation and propagation is observed. Figure 12 displays uniform crack initiation from multiple sites corresponding to the FSW tool shoulder's markings causing lap defects on the weld's top surface (weld edge, RT side). Multiple sites of crack initiation are indicated with the arrows. A magnified view of a typical lap defect is shown in Figure 13. The lap defect is observed continuously along the weld length but with varying intensity and depth.

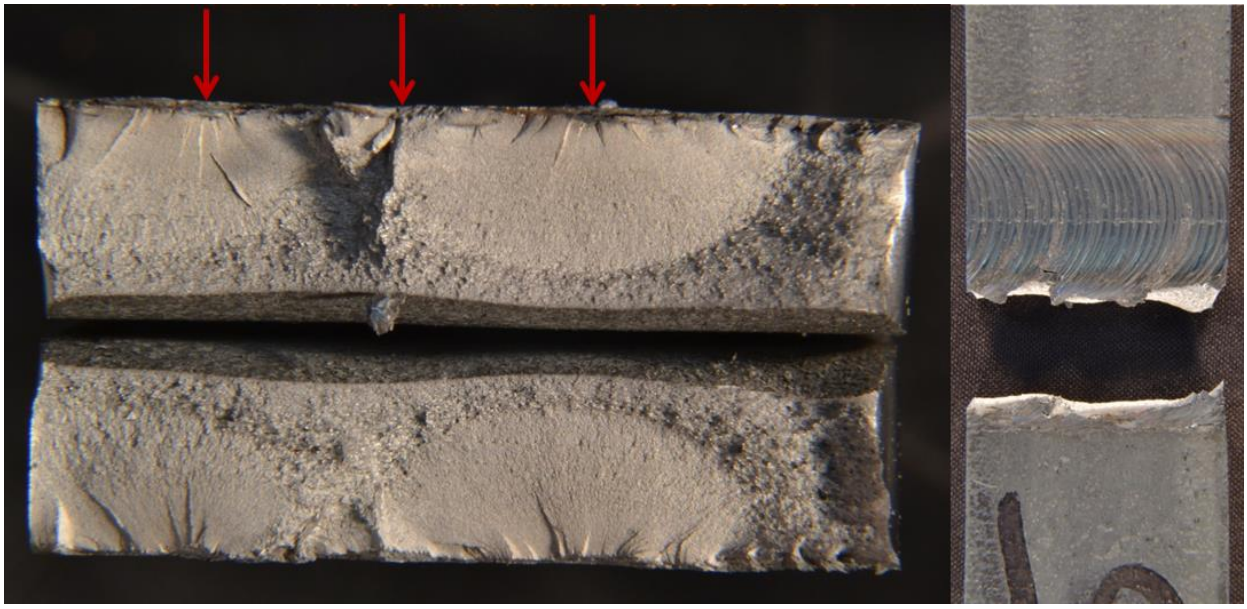

Figure 12. Typical fracture surface of intermediate weld specimens

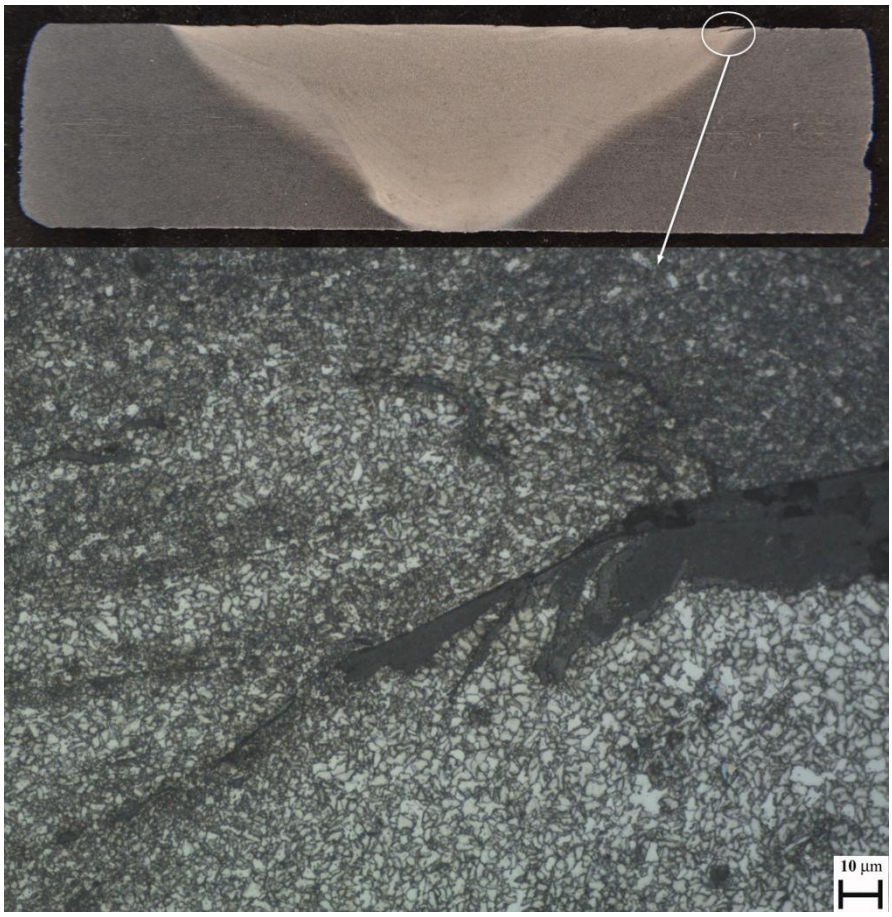

Figure 13. Intermediate weld, RT side top surface [x500, Etched]

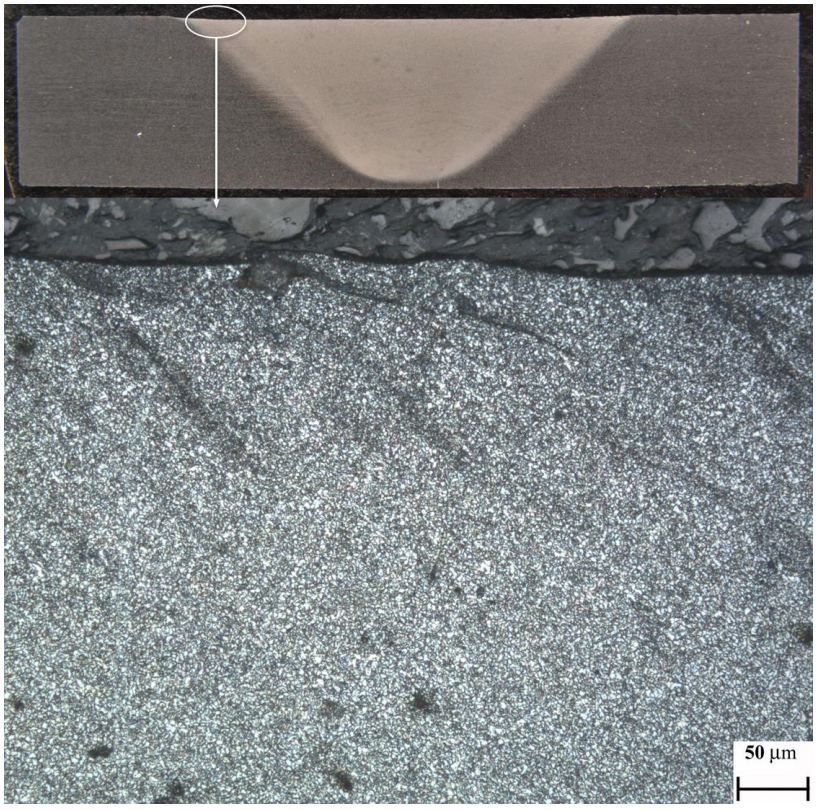

Figure 14. Slow weld, AD side top surface [x200, Etched]

Another possible crack initiation site was observed in the failed slow speed specimens; cracks originated from incomplete fusion paths containing interconnected non-metallic inclusions on the AD side (Figure 14). The fracture path is seen to have propagated through the TMAZ and subsequently into the parent material in a plane nearly perpendicular to the top surface (Figure 15); two more incomplete fusion paths from which cracks did not propagate are marked in Figure 15.

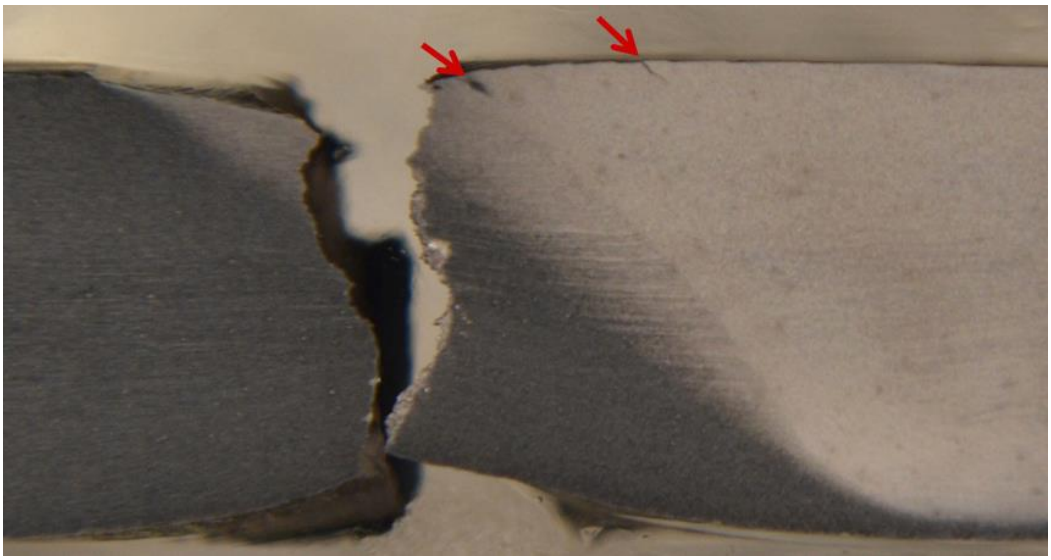

Figure 15. Macrograph of slow weld specimen's fracture path (side view) [Etched]

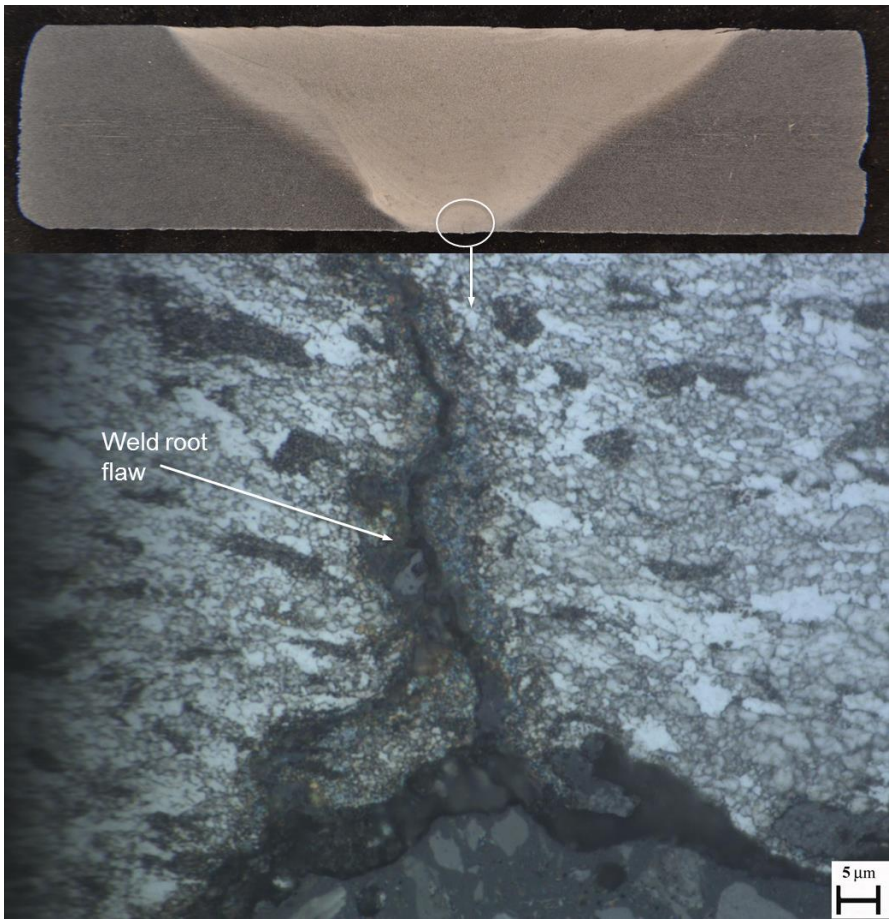

Figure 16. Fast weld, root flaw at high magnification [x1000, Etched]

Five of the fast weld specimens failed from the weld root flaw; intermittent insufficient fusion at the weld root occurred during the FSW process, i.e. a weld root flaw (Figure 16). The remaining three fast weld specimens failed through uniform crack initiation from the tool shoulder's markings on the weld top surface (laps), in a manner comparable to the intermediate weld specimens above; the corresponding fracture path is illustrated in Figure 17.

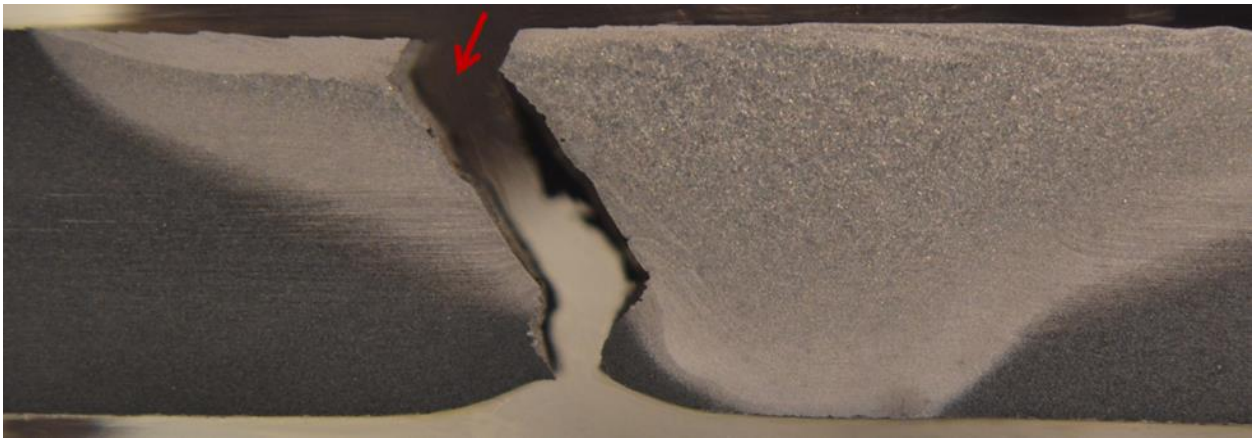

Figure 17. Macrograph of fast weld specimen's fracture path (side view) [Etched]

4.1. Effect of surface lap defect

It has been determined in Sections 3 and 4 that the main reason for crack initiation in friction stir welds produced at the optimal intermediate speed is the lap defect introduced by the FSW tool shoulder. Microstructural observations and subsequent measurements on the captured micrographs (Figure 13) showed that the deepest top surface lap defect found is approx. 0.45 mm. To assess the effect of the surface lap defect on the FSW fatigue performance, three intermediate speed specimens were fatigue tested under a stress range of 90% of YS following grinding. The grinding consisted of removal of a 0.5 mm layer from the weld top surface. The specimens were polished after grinding.

For these specimens, the fatigue tests were terminated at or above 3.2×10^6 cycles; no evidence of fatigue cracking was present. In agreement with previous publications in aluminium [9,27] and steel [28] FSW, this confirms that the top surface processing features generated by the FSW tool are responsible for fatigue cracks in the intermediate speed FSW and indicates a potential way to improve the fatigue performance by reducing or eliminating the top surface markings produced by the tool.

5. Conclusions

An experimental programme of fatigue performance assessment of friction stir butt welds produced from 6 mm thick marine grade DH36 steel was undertaken to develop novel *S-N* curve parameters. The main focus of the programme was fatigue testing accompanied by tensile tests, geometry measurements, hardness and residual stress measurements, and fracture surface examination. The effect of varying welding parameters was also investigated.

Analysis of the fatigue testing results showed that the fatigue resistance of FSW butt joints is well above the weld detail class of the IIW for single side fusion welded butt joints. The *S-N* curve for the intermediate welding speed was constructed; it has been demonstrated that this *S-N* curve has a shallower slope than the one recommended by IIW for fusion welds, thus concluding that the slope recommended by IIW is not applicable to FSW. The newly developed

S-N curve for friction stir butt welded joints in low alloy steel is an important outcome from this study. In addition, the design fatigue strength at $2x10^6$ cycles is above the parent material *S-N* curve FAT160 (m=5) [3], hence confirming that the use of the intermediate weld is the most appropriate for the derivation of the *S-N* curve. Moreover, the slow welding speed was found to result in better fatigue performance. This is because the slow speed produces a highly refined, homogeneous and defect-free microstructure as reported in a prior study [15].

Residual stress measurements were recorded using the X-Ray diffraction technique. It was established that, although the location of the maximum transverse residual stress was found in the central stir zone of the weld, the typical crack initiation site was observed at the retreating side of the weld edge resulting from the processing features generated by the friction stir welding tool. Since the maximum transverse residual stress and crack initiation sites are unrelated, the fatigue performance of FSW is improved compared to fusion welding where the maximum transverse residual stress and the edge of the weld toe coincide.

Examination of fracture surfaces where surface breaking flaws were present highlighted the critical importance of the lap defect in relation to fracture initiation. Fatigue testing of specimens without top surface defects resulted in a substantial improvement in fatigue life thus exhibiting that the markings produced by the FSW tool shoulder are responsible for crack initiation. It is important to emphasize that despite the presence of minor surface breaking flaws within the TMAZ, the overall fatigue strength is still considerably higher than the weld detail class of FAT 80.

Acknowledgements

The authors gratefully acknowledge the financial support of the European Union which has funded this work as part of the Collaborative Research Project HILDA (High Integrity Low Distortion Assembly) through the Seventh Framework Programme (SCP2-GA-2012-314534-HILDA), in addition to financial support provided by the Lloyd's Register Foundation.

References

[1] Maddox SJ. Fatigue design rules for welded structures. Prog Struct Eng Mater 2000;2:102–9.

[2] IACS. Common Structural Rules for Bulk Carriers and Oil Tankers. 2014.

[3] Hobbacher A. Draft: Recommendations for Fatigue Design of Welded Joints and Components. International Institute of Welding, XIII-2460-13. 2013.

[4] Fricke W. Fatigue analysis of welded joints: state of development. Mar Struct 2003;16:185–200.

[5] Thomas WM, Nicholas ED, Needham JC, Murch MG, Temple-Smith P, Dawes CJ. Friction welding. PCT/GB92/02203, 1991.

[6] Barsoum Z, Khurshid M, Barsoum I. Fatigue strength evaluation of friction stir welded aluminium joints using the nominal and notch stress concepts. Mater Des 2012;41:231–8.

[7] Uematsu Y, Tokaji K, Shibata H, Tozaki Y, Ohmune T. Fatigue behaviour of friction stir welds without neither welding flash nor flaw in several aluminium alloys. Int J Fatigue 2009;31:1443–53.

[8] Ericsson M, Sandstrom R. Influence of welding speed on the fatigue of friction stir welds, and comparison with MIG and TIG. Int J Fatigue 2003;25:1379–87.

[9] Pedemonte M, Gambaro C, Lertora E, Mandolfino C. Fatigue assessment of AA 8090 friction stir butt welds after surface finishing treatment. Aerosp Sci Technol 2013;27:188–92.

[10] McPherson N, Galloway A, Cater S, Hambling S. Friction stir welding of thin DH36 steel plate. Sci Technol Weld Join 2013;18:441–50.

[11] Baillie P, Campbell S, Galloway A, Cater S, Mcpherson N. A Comparison of Double Sided Friction Stir Welding in Air and Underwater for 6mm S275 Steel Plate. Int J Chem Nucl Metall Mater Eng 2014;8:651–5.

[12] Azevedo J, Infante V, Quintino L, dos Santos J. Fatigue Behaviour of Friction Stir Welded Steel Joints. Adv Mater Res 2014;891-892:1488–93.

[13] Lakshminarayanan AK, Balasubramanian V. Assessment of fatigue life and crack growth resistance of friction stir welded AISI 409M ferritic stainless steel joints. Mater Sci Eng A 2012;539:143–53.

[14] Lloyd's Register. Rules for the Manufacture, Testing and Certification of Materials. London: 2014.

[15] Toumpis A, Galloway A, Cater S, McPherson N. Development of a process envelope for friction stir welding of DH36 steel – A step change. Mater Des 2014;62:64–75.

[16] Toumpis A, Galloway A, Polezhayeva H, Molter L. Fatigue Assessment of Friction Stir Welded DH36 Steel. Frict. Stir Weld. Process. VIII, Orlando, FL: 2015.

[17] British Standards Institution. BS 7270. Metallic materials – Constant amplitude strain controlled axial fatigue – Method of test. London: 2006.

[18] Radaj D, Sonsino CM, Fricke W. Fatigue Assessment of Welded Joints by Local Approaches. 2nd ed. Cambridge: Woodhead Publishing; 2006.

[19] Hilley ME, editor. Residual Stress Measurement by X-ray Diffraction - SAE J784a. Warrendale, PA: Society of Automotive Engineers; 1971.

[20] Maddox SJ. Fatigue Strength of Welded Structures. 2nd ed. Cambridge: Woodhead Publishing; 2002.

[21] Vuhereer T, Maruschak P, Samardzic I. Behaviour of coarse grain heat affected zone (HAZ) during cycle loading. Metalurgija 2012;51:301-4.

[22] Fitzpatrick ME, Fry AT, Holdway P, Kandil FA, Shackleton J, Suominen L. Measurement Good Practice Guide No. 52. Determination of residual stresses by X-ray diffraction. Teddington: 2005.

[23] Maddox SJ, Dore MJ, Smith SD. Investigation of ultrasonic peening for upgrading a welded steel structure. XIII-2326-10. Istanbul: International Institute of Welding: 2010.

[24] Ahmad B, Fitzpatrick ME, Howarth D, Polezhayeva H, Przydatek J, Robinson A. Residual stress measurements and fatigue testing of butt welds subjected to peening treatments. XIII-2497-13. International Institute of Welding: 2013.

[25] Schneider CRA, Maddox SJ. Best Practice Guide on Statistical Analysis of Fatigue Data. International Institute of Welding, XIII-WG1-114-03. Cambridge: 2003.

[26] Barsoum Z, Marquis GB. Draft: Recommendations on Techniques for Improving the Fatigue Strength of Welded Components and Structures. International Institute of Welding, XIII-WG2-140-12.

[27] Lomolino S, Tovo R, dos Santos J. On the fatigue behaviour and design curves of friction stir butt-welded Al alloys. Int J Fatigue 2005;27:305–16.

[28] Toumpis A, Galloway A, Molter L, Polezhayeva H. Systematic investigation of the fatigue performance of a friction stir welded low alloy steel. Mater Des 2015;80:116–28.